



저작자표시-비영리-변경금지 2.0 대한민국

이용자는 아래의 조건을 따르는 경우에 한하여 자유롭게

- 이 저작물을 복제, 배포, 전송, 전시, 공연 및 방송할 수 있습니다.

다음과 같은 조건을 따라야 합니다:



저작자표시. 귀하는 원저작자를 표시하여야 합니다.



비영리. 귀하는 이 저작물을 영리 목적으로 이용할 수 없습니다.



변경금지. 귀하는 이 저작물을 개작, 변형 또는 가공할 수 없습니다.

- 귀하는, 이 저작물의 재이용이나 배포의 경우, 이 저작물에 적용된 이용허락조건을 명확하게 나타내어야 합니다.
- 저작권자로부터 별도의 허가를 받으면 이러한 조건들은 적용되지 않습니다.

저작권법에 따른 이용자의 권리는 위의 내용에 의하여 영향을 받지 않습니다.

이것은 [이용허락규약\(Legal Code\)](#)을 이해하기 쉽게 요약한 것입니다.

[Disclaimer](#)

Master of Science

Investigation of the genes associated with VSIG4-mediated
T cell inhibition using genome-wide CRISPR knockout
screenings

The Graduate School
of the University of Ulsan
Department of Medical Science
Seongfeel Jeong

Investigation of the genes associated with VSIG4-mediated
T cell inhibition using genome-wide CRISPR knockout
screenings

Supervisor: Chan-Sik Park

A Dissertation

Submitted to

the Graduate School of the University of Ulsan

In partial Fulfillment of the Requirements

for the Degree of

Master of Science

by

Seongfeel Jeong

Department of Medical Science

University of Ulsan, Korea

August 2023

Investigation of the genes associated with VSIG4-mediated
T cell inhibition using genome-wide CRISPR knockout
screenings

This certifies that the master's thesis of

Seongfeel Jeong is approved.



Committee Chair Dr. Hyung-Seung Jin



Committee Member Dr. Chan-Sik Park



Committee Member Dr. Hyo-Kyung Pak

Department of Medical Science

University of Ulsan, Korea

August 2023

Acknowledgements

Firstly, I would like to thank my advisor professor Chan-Sik Park. He provided me with the environment to conduct various experiments and the opportunity to improve myself through continuous discussion.

Next, I would like to express my gratitude to my advisors Hyo-Kyung Pak, Jin Roh and Hyung-Seung Jin. They provided me with lots of valuable advice and helped me broaden my insight. I also appreciated the encouragement from the members of our lab.

Finally, I would like to express gratitude to my family for their dedication in making me who I am. Their constant support, sacrifices, and guidance have played a significant role in my personal and academic growth.

Abstract

The blockade of immune checkpoint molecules that suppress T cell activation has demonstrated improved therapeutic efficacy, durable response, and safety. However, the limited therapeutic efficacy and the low response rates of these immunotherapies in various types of cancer have motivated us to explore new immune checkpoint molecules. VSIG4, a novel immune checkpoint molecule, suppresses T cell activity and promotes the differentiation of regulatory T cells. Its expression indicates a significant correlation with age-related immune diseases and is strongly associated with the prognosis of gastric cancer and lymphoma. Although it has therapeutic potential, the T cell inhibition mechanism of VSIG4 has not been comprehensively understood so far. Here, we investigated the VSIG4 signaling pathway that inhibited T cell activation by the genome-wide CRISPR knockout screening, based on the CD69 induction, a well-known marker for T cell activation. Our results showed that VSIG4 can regulate ribosomal RNA processing, CD5 signaling pathway, and S1PR1 signaling pathway for the regulation of T cell activation. These mechanisms are known to be associated

with regulating the signal strength of T cell receptors, the differentiation of regulatory T cells, and the activation of T cells. Our results provide the basis for developing therapeutic approaches for age-related immune diseases, gastric cancer, and lymphoma. The distinct T cell inhibition mechanism of VSIG4 will meet the unmet needs of patients who did not respond to conventional immune checkpoint blockade therapy.

Contents

Approval page

Acknowledgements

Abstract (English)..... i

Contents iii

List of figures and tables vi

1. Introduction 1

1-1. Immune checkpoint molecules..... 1

1-2. V-set and immunoglobulin domain – containing 4 3

1-3. Genome-wide CRISPR knockout screening 5

2. Materials & Methods	13
2-1. Cell culture	13
2-2. Cryopreservation of cells	14
2-3. T cell activation	15
2-4. Western blot	15
2-5. Gel extraction	18
2-6. Lentiviral production and transduction	19
2-7. Human genome-wide CRISPR knockout screening	22
3. Result	34
3-1. Establishment of functional Cas9-expressing Jurkat cell line...	34
3-2. Amplification of human genome-wide CRISPR knockout library	35

3-3. Enriched sgRNA amplification of activated sgRNA⁺ Cas9	
Jurkat cell	36
3-4. Control Ig-treated group showed enrichment of sgRNAs	
associated with TCR signaling regulators	37
3-5. CRISPR screening reveals candidate genes of T cell inhibition	
mechanism of VSIG4	38
4. Discussion	54
5. Conclusion	58
6. References.....	59
Abstract (in Korean)	64

List of figures and tables

1. Introduction

Figure 1-1. Illustration of T cell inhibition by VSIG4.....7

Figure 1-2. Workflow of genome-wide CRISPR knockout screening.....9

Figure 1-3. Experimental strategy for this screening11

2. Materials & Methods

Table 2-1. Primer sequences for amplification of sgRNAs of library32

Table 2-2. PCR master mix for amplification of sgRNAs in library33

Table 2-3. Cycling condition for PCR33

3. Result

Figure 3-1. Establishment of functional Cas9-expressing Jurkat cell line.40

Figure 3-2. Amplification of human genome-wide CRISPR Knockout library .42

**Figure 3-3. Enriched sgRNA amplification based on CD69 expression on
activated sgRNA⁺ Cas9 Jurkat cell44**

**Figure 3-4. Control Ig-treated group showed enrichment of sgRNAs associated
with TCR signaling regulators47**

**Figure 3-5. CRISPR screenings revealed candidate genes of T cell inhibition
mechanism of VSIG449**

Table 3-1. Enriched pathway of VSIG4 Ig-treated CD69⁺ group51

**Table 3-2. The positive rank of triple hit genes in VSIG4 Ig-treated CD69⁺
group53**

1. Introduction

1.1 Immune checkpoint molecules

Numerous therapeutic approaches have been devised to enhance T cell immune responses by targeting specific molecules, as cancer cells can diminish T cell activity to evade immune surveillance.¹ Immune checkpoint molecules, which negatively regulate the T cell activation, have become important targets for cancer immunotherapy. The immune checkpoint molecules maintain immune homeostasis by binding their receptors or ligands². These interactions within the cancer environment suppress the T cell activation and induce immune tolerance to evade the immune response. Immune checkpoint blockade (ICB), which disrupts the receptor-ligand interaction of immune checkpoint molecules, has been used for cancer immunotherapy. As the ICB targeting Programmed cell death protein 1 (PD-1) and Cytotoxic T-lymphocyte-associated protein 4 (CTLA-4) has received much attention because of their promising result³. The PD-1 and CTLA-4 blockade have shown increased survival of patients in many cancer

types and increased overall survival rates⁴. In the PD-1 blockade therapy across multiple cancer types, the overall survival rate of 76% at 3 years and 63% at 5 years were observed in responders⁵. However, the proportion of patients who responded to the treatment was below 30%. Moreover, many patients experienced immunotoxicity as a side effect.

Recently, second-tier immune checkpoint molecules such as T cell immunoglobulin and mucin domain-containing protein 3 (TIM-3) and T-cell immunoglobulin and ITIM domain (TIGIT)⁶, which showed a tissue-specific expression and a cell type-specific stimulation, have gained attention. These molecules have demonstrated the low toxicity and the improved therapeutic efficacy because of their specificity. Despite investigations of various immune checkpoint molecules, the efficacy of ICB remains insufficient. To enhance efficacy of the therapy, the combination of PD-1 and CTLA-4 blockade has been studied and reported the significantly increased objective response rate (61% with combination therapy compared to 11% with CTLA-4 blockade) and the improved overall survival (above 50% with combination therapy) in melanoma patients⁷⁻⁹. Recent studies have shown that many immune checkpoint molecules have distinct signaling transduction mechanisms¹⁰. In this respect, deeper

understandings of the signal transduction mechanism of each immune checkpoint molecule are important to improve efficacy of the combination ICB therapy.

1.2 V-set and immunoglobulin domain-containing 4

V-set and immunoglobulin domain-containing 4 (VSIG4), a B7 family-related protein, is a novel second-tier immune checkpoint molecule. VSIG4 is known as a receptor for C3b and induces clearance mediated by VSIG4 of C3b-opsonized pathogens^{11,12}. VSIG4 is a transmembrane receptor located on the X chromosome in human. The longest isoform of human VSIG4, comprising 399 amino acids, has been extensively investigated. It is composed of five distinct domains: an extracellular signal peptide, IgV domain, IgC2 domain, transmembrane domain, and intracellular sequence¹³. VSIG4 is predominantly expressed in tissue-restricted macrophages and is associated with the inhibition of T cell activation by binding to an unknown receptor on T cells.¹³⁻¹⁵ The expression of this receptor for VSIG4 is induced during the early activation of CD4 and CD8 T cells¹⁶. VSIG4 induces peripheral

immune tolerance by suppressing the proliferation and the cytokine production of CD4 and CD8 T cells¹⁷. Additionally, VSIG4 promotes the differentiation of TGF- β induced Treg (iTreg) and stabilizes the expression of FOXP3 in iTreg¹⁸. Collectively, VSIG4 is the important regulator of T cell immunity as an immune checkpoint molecule (Fig. 1-1).

A recent study reported that the increased VSIG4 expression is associated with poor prognosis in some types of cancer, including gastric cancer¹⁹, lung carcinoma²⁰, ovarian cancer²¹, and multiple myeloma²². Especially, advanced gastric cancer lacks significant treatment options. In contrast to other immune checkpoint molecules, there is a strong correlation between the expression level of VSIG4 in advanced gastric cancer tissue and the survival rate¹⁹. In a recent study, an aging macrophage upregulates the expression of VSIG4, this macrophage induces age-related systemic inflammation and immunosenescence²³.

Taken together, VSIG4 seems to be the most crucial therapeutic target for cancer and immune diseases. Although it has the potential, the mechanism of VSIG4 is not understood. To develop efficient therapies, a comprehensive understanding by investigating the T cell inhibition mechanism of VSIG4 is essential.

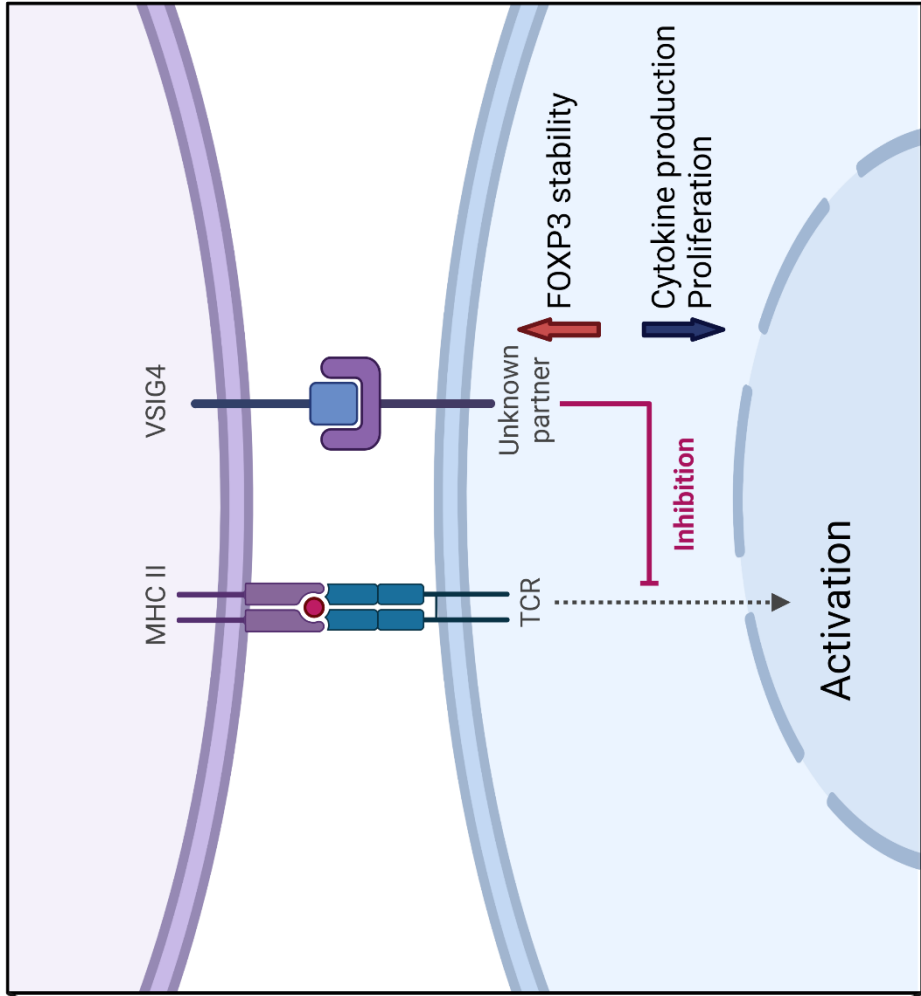
1.3 Genome-wide CRISPR knockout screening

Clustered regularly interspaced short palindromic repeats (CRISPR)/ CRISPR-associated endonuclease 9 (Cas9) system is an adaptive immune system found in *Staphylococcus pyogenes*, it functions to restrict foreign DNA. This system consists of Cas9 and guide RNA (gRNA), which comprises tracrRNA and crRNA. The Cas9 protein is guided by the tracrRNA of gRNA to target a specific sequence of a gene forming a base pair with the crRNA of gRNA. After that, a catalytic domain of Cas9 causes a double-strand break of the target gene. Using this mechanism, the CRISPR/Cas9 system has been used as a gene-editing tool in various fields ²⁴. Genome-wide CRISPR knockout screening has been applied to identify genes involved in specific biological processes. Here we applied a genome-wide CRISPR knockout screening to investigate VSIG4-mediated T cell inhibition mechanism in Jurkat E6-1 cell line (Fig. 1-2), which is commonly used for the investigation of T cell signaling. By analyzing the VSIG4 Ig-treated CD69⁺ population that has impaired T cell inhibition function of VSIG4 by sgRNA (Fig 1-3), we revealed 29 candidate genes and pathways associated with the T cell inhibition mechanism of VSIG4.

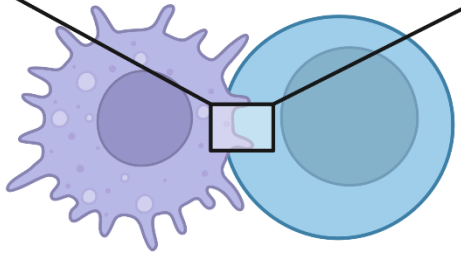
Aim of the investigation

To elucidate the T cell inhibition mechanism of the novel immune checkpoint molecule, VSIG4 and provide a basis for novel therapeutic strategies, we conducted the genome-wide CRISPR knockout screenings in Jurkat T cells.

T cell inhibition via VSIG4



Tissue restricted macrophage



T cell

Figure 1-1. Illustration of T cell inhibition by VSIG4. The expression of VSIG4 on tissue-restricted macrophage induces stabilization of the expression of FOXP3 and inhibits the T cell activation, including proliferation and cytokine production. This inhibition occurs through the interaction between an unidentified receptor on the T cell and VSIG4. Figure created with biorender.com.

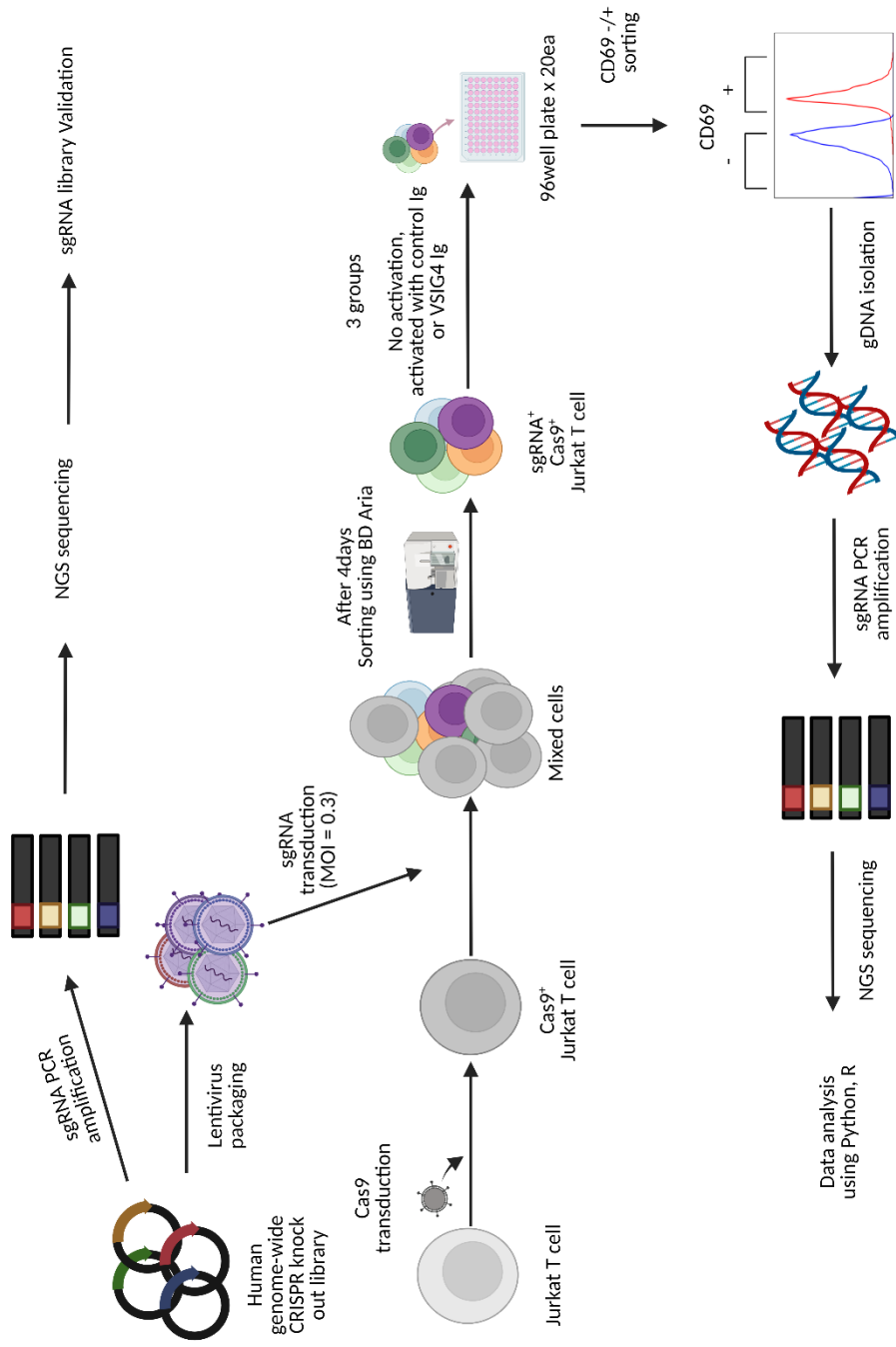
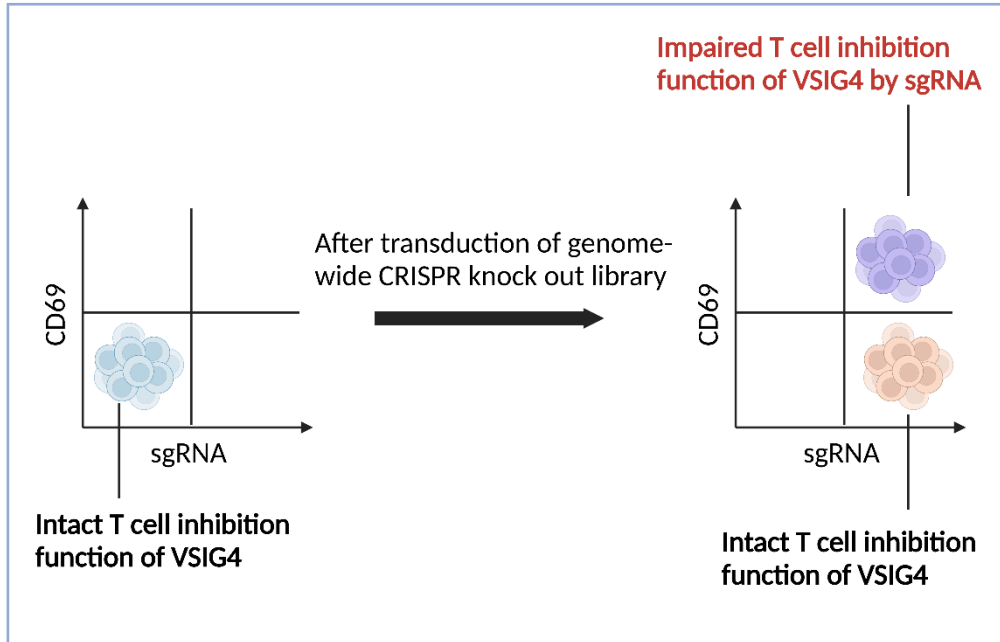


Figure 1-2. Workflow of genome-wide CRISPR knockout screening. sgRNA library for genome-wide CRISPR knockout screening was amplified. The lentiviral library was produced by lentiX-293T cells and transduced to Cas9 Jurkat cells at MFI 0.3. The library transduced Cas9 Jurkat cells were sorted and cultured. 7 days after, the transduced Cas9 Jurkat cells were activated with super engaged control Ig or VSIG4 Ig, were harvested. The no activated sample was also harvested. The harvested cells were sorted by CD69 expression and the gDNA was isolated from the harvest cells. The sgRNA on gDNA was amplified and sequenced. The sequenced sgRNA data was analyzed using R and Python. Figure created with biorender.com.

Target population of this screening



Mechanism of VSIG4 Ig treated CD69⁺ population

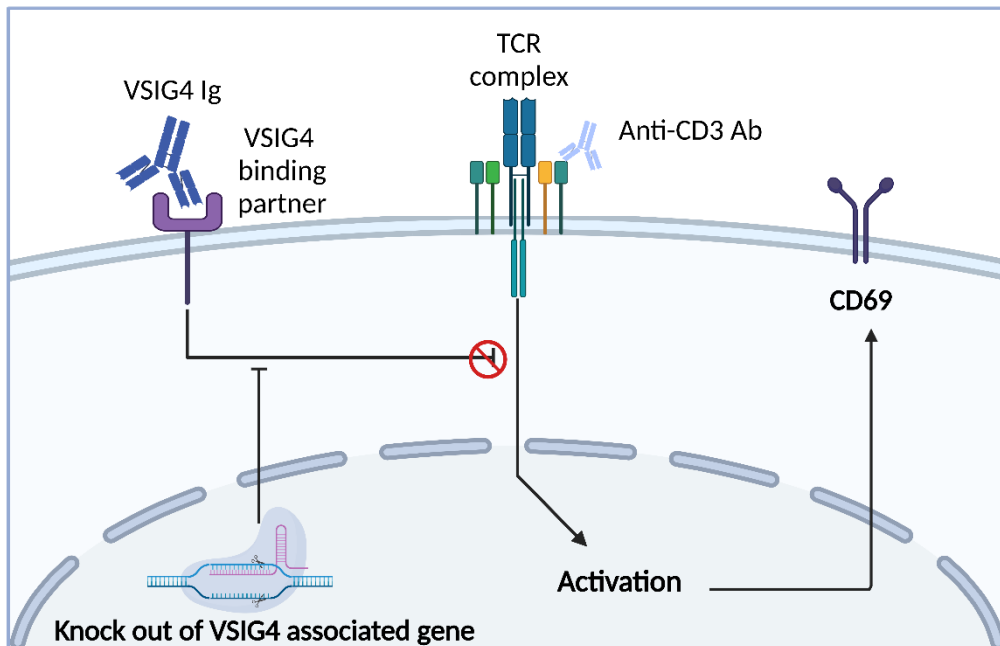


Figure 1-3. Experimental strategy for this screening. The upper image shows the target population has impaired T cell inhibition function of VSIG4 by sgRNA. This population shows the phenotype expressing CD69⁺, despite the treatment of VSIG4. The lower image shows the mechanism of this screening. Figure created with biorender.com.

2. Materials & Methods

2-1. Cell culture

2-1-1. Jurkat T cells

Jurkat T cells (clone E6-1) were obtained from American type culture collection. Jurkat T cells were cultured in Roswell Park Memorial Institute -1640 media (Hyclone, # SH30027.01) containing 10% fetal bovine serum (Gibco, # 16000044) and 100 µg/mL of antibiotic-antimycotic (Gibco, #15240062). Jurkat T cells were cultured at a density between $2-10 \times 10^5$ cells/mL, grown in a T flask and stored at 37°C incubator with 5% of CO₂ atmosphere condition. Cells were subcultured once every 2 days.

2-1-2. Lenti-X 293T

Lenti-X 293T cells (Takara Bio, #632180) were obtained. 293T cells were cultured in DMEM/High glucose with L-glutamine, sodium pyruvate (Hyclone, #SH30243.01) media containing 10% FBS and 100 µg/mL of antibiotic-antimycotic. 293T cells were seeded with a

density of 2×10^5 cells on a 100 π dish. When the confluency of 293T cells reached 80%, cells were subcultured. For subculturing, the cells were washed with PBS and then treated with trypsin-EDTA (0.2%), phenol red (Gibco, # 25200072), and incubated for 5 min at 37°C incubator. For neutralizing trypsin-EDTA solution, the harvested cells were 1:3 diluted using culture media. After cell counting, 3×10^5 cells of the cells were harvested, and centrifuged at 300 g for 3 min. The cell pellet was suspended with culture media, the suspended cells were seeded in a 100 π dish and then stored at 37°C with 5% of CO₂ atmosphere condition.

2-2. Cryopreservation of cells

Cells were harvested by twice subculture cell number and resuspended with 1 mL of FBS containing 10% DMSO. The cells were transferred to a cryotube, the tubes were placed in a NALGENE cryo 1°C freezing container (Thermo Scientific, #5100-0036) with isopropanol and then stored at 80°C for 1 day. The next day, the tubes were stored in a liquid nitrogen container.

2-3. T cell activation

For T cell activation, 96-well plates were coated overnight at 4°C with 100 µL of cold PBS containing 1 µg/mL of CD3 Monoclonal Antibody (eBioscience, #16-0036-85, clone SK7).

After one day, the wells were washed twice with 250 µL of PBS. Jurkat T cells were harvested, centrifuged at 300 g for 3 min and resuspended to a final concentration of 5×10^5 cells/mL in culture media, containing soluble 10 µg/mL of control Ig (eBioscience, #16-4724-85) or VSIG4-mouse Fc fusion protein (VSIG Ig). VSIG4 Ig was a gift from Professor In-Hak Choi's laboratory of Inje University. For antibody engagement, 10 µg/mL of AffiniPure Goat Anti-Mouse IgG + IgM (H+L) (Jackson ImmunoResearch, #115-005-044) was treated. After that, 200 µL of cells were seeded in each well and incubated for 8 hours at 37°C with 5% of CO₂.

2-4. Western blot

2-4-1. Sample preparation

Cells were harvested 2×10^6 cells and washed twice with PBS, the cell pellets were resuspended lysis buffer (Cell signaling technology, # 9803) containing protease inhibitor (Roche, #11697498001) and phosphatase inhibitor (Roche, #4906845001). The cells were lysed for 30 min on ice and the lysates were centrifuged for 30 min at 12,000 g and 4°C. The supernatants were harvested and quantified total protein amount using Bicinchoninic Acid (BCA) assay. 20 µg of lysates were added 4x Laemmli buffer (Bio-Rad, #1610747) containing 10% β-mercaptoethanol (Sigma-Aldrich, #M6250) and boiled at 98°C for 5 min.

2-4-1-1. BCA assay

Working reagents were prepared by mixing 50 parts of Pierce™ BCA Protein Assay Reagent A (Thermo Scientific, #23228) with 1 part of Pierce™ BCA Protein Assay Reagent B (Thermo Scientific, #23224). 100 µL of working reagent was pipetted into each well of a 96-well plate. After that 100 µL of BSA standard or the samples were added, mixed, and incubated at 37°C. Finally, the plates were measured the absorbance at 562 nm on a Sunrise™ absorbance reader (Tecan, #30190079) and the total protein amount was calculated.

2-4-2. Gel electrophoresis and transfer

4–15% Mini-PROTEAN® TGX™ Precast Gel (Bio-Rad, # 4561083EDU) was used. 20 µg of protein lysate was loaded on each well and separated by electrophoresis at 120 volts for 45 min. The protein contained gel and PVDF membrane (Bio-Rad, # 1620284) were located together with 3M paper (Bio-Rad, # 1703932) between sponges. After that the proteins were transferred in a transfer buffer at 300 mA for 2 hours. The transfer buffer was made using a 10X transfer buffer containing 2.5mM tris, 192mM glycine and 1L DW. The 10X transfer buffer was diluted at the ratio of DW: methanol: 10X transfer buffer = 7: 2: 1.

2-4-3. Protein detection

The PVDF membrane containing proteins was washed with TBS-T buffer (Biosesang, #T2007P). After washing, the membrane was incubated for 1 hour with a blocking buffer (TBS-T with 5% Powdered milk (Carl Roth, #68514-61-4)) to prevent non-specific binding of antibodies. After 1 hour incubation, the buffer was disposed, and then the membrane was incubated at 4°C overnight with 9 µL of primary antibody in 9 mL of blocking buffer. The

next day, the primary antibody contained solution was discarded. The membrane was washed three times using TBS-T. The washed membrane was incubated with 3 μ L of secondary antibody in 9 mL of TBS-T at room temperature for 2 hours. The membrane was washed three times using TBS-T and incubated with SuperSignal™ West Pico PLUS Chemiluminescent Substrate (Thermo Scientific, #34580) for 5 min. The membrane was imaged by imageQuant LAS4000 (GE healthcare, #28-9558-10). After imaging, the membrane was incubated with a stripping buffer (Thermo Scientific, #46430) for 1 hour to detach bounded antibodies.

2-5. Gel extraction

2-5-1. Preparation of samples

The DNA sample was run on 2% agarose (GenDEPOT, # A0224-050) in TBE buffer (Biosesang, # TR2004-100-00) gel. The sample was loaded in the gel and electrophoresis was conducted at 135 volts for 45 minutes. The band was cut by the blade and collected 15 mL tube.

2-5-2. Gel extraction

NucleoSpin® Gel and PCR Clean-up (Macherey-Nagel, #740609) was used. 200 µL of buffer NT1 per 100mg of agarose gel was added into the tube and incubated at 50°C for 10 min with 300 rpm. For DNA binding, the dissolved PCR product was placed into a column and loaded up to 700 µL. This step was repeated until the sample was used up. For washing the membrane, buffer NT3 was added to the column and centrifuged at 11,000 g for 30 sec. This washing step was repeated. To dry the membrane, the column was centrifuged at 11,000 g for 1 min. The dry column was placed into a 1.5 mL microcentrifuge tube. 30 µL of buffer NE was added and incubated at room temperature for 5 min. After the incubation, the tube was centrifuged at 11,000 g for 1 min. The eluted DNA was quantified and stored at – 20°C.

2-6. Lentiviral production and transduction

2-6-1 Vector information

2-6-1-1 pMD2.G, psPAX2

pMD2.G was a gift from Didier Trono (Addgene, #12260). pMD2.G is a VSV-G envelope expressing plasmid. psPAX2 was a gift from Didier Trono (Addgene, #12260). psPAX2 is a lentiviral packaging plasmid that has Gag and Pol genes.

2-6-1-2 LentiCas9-Blast

LentiCas9-Blast was a gift from Feng Zhang (Addgene, #52962)²⁵. lentiCas9-Blast has a lentiviral backbone. It expresses *Streptococcus pyogenes* Cas9 (spCas9) protein that has human optimized codon. The selectable marker of this plasmid is blasticidin.

2-6-1-3 pKLV2-U6gRNA5(gGFP)-PGKBFP2AGFP-W

pKLV2-U6gRNA5(gGFP)-PGKBFP2AGFP-W was a gift from Kosuke Yusa (Addgene #67980)²⁶. This plasmid expresses GFP, BFP and guide RNA of GFP (gGFP). The expressed gGFP forms an RNP complex with spCas9 in the spCas9 expressing cell line, and then perturbate the GFP gene. The BFP-expressing cell has functional spCas9, whereas the BFP and GFP-expressing cell have dysfunctional spCas9.

2-6-1-4 Human Improved Genome-wide Knockout CRISPR Library

Human Improved Genome-wide Knockout CRISPR Library v1 was a gift from Kosuke Yusa (Addgene, #67989)²⁶, the library consists of 90,709 guide RNA sequences targeting 18,010 human genes for genome-wide knockout CRISPR screening. The expression marker of this plasmid is BFP.

2-6-2 Lentiviral production and transduction

Three days before lentiviral production, Lenti-X 293T cells were seeded with a density of 5×10^6 cells/10 mL of culture media in a 150T flask. After 2 days, the 293T cells were harvested and seeded with a density of 5×10^6 cells / 10 mL of culture media in 100π dish each. The cells were incubated at 37 °C, 5% CO₂ for ~20 hours. When the confluency of 293T cells reached 80%, psPAX2, pMD2.G and expression vectors were diluted 1 μg, 1 μg and 4 μg / 10 μL each using DW for one dish. After dilution, 1 μg of psPAX2 and pMD2.G vector, and 4 μg of expression vector were mixed in 1 mL of Opti-MEM™ I Reduced Serum Medium (Gibco, #32985062) and then vortexed gently. Trans-IT 293 transfection reagent (Mirus Bio, #MIR

2704) was added to Opti-MEM media with vectors, vortexed gently and incubated at RT for 30 minutes. During the incubation, the cell culture media was changed to 5 mL of fresh Opti-MEM media. After the incubation, mixture of Trans-IT 293 transfection reagent and vectors complex was added dropwise to different areas of the dish. The cells were incubated at 37°C, 5% CO₂ for 1 day and changed the media to fresh Opti-MEM media. After 3 days, the culture soup was harvested and centrifuged at 300 g for 3 min. The supernatant was loaded to a 50 mL syringe and filtered using a 40 µm filter. For concentration of the virus, the filtered virus soup was centrifuged at 4°C, 16500 rpm, for 90 min. The supernatant was aspirated, the virus pellet was resuspended in PBS. The viruses were stored at -80°C.

2-7. Human genome-wide CRISPR knockout screening

2-7-1. Establishing functional Cas9 Jurkat cell line

To establish the Cas9 Jurkat T cell line, Jurkat E6-1 cells were cultured at density 2×10^6 cells in 10 mL. Hexadimethrine bromide was added to culture media at 8 µg/mL and then the cells

were pipetted. Subsequently, 100 μ L of a Cas9 lentivirus was added, and the cells were mixed well and incubated 24 hours at 37°C in 5% CO₂. After 1 day, the culture media was changed to fresh media. Cas9-transduced Jurkat T cells were cultured at a density between 2-10 x 10⁵ cells/mL. After 7 days, the Cas9 transduced Jurkat cells were selected using blasticidin 10 μ g/mL for 2 weeks. After that, Cas9 expression and functional test of the Cas9 Jurkat cells were analyzed by western blot. For the functional test of Cas9, the Cas9 Jurkat cells were cultured at density 2 x 10⁶ cells in 10 mL. Hexadimethrine bromide was added to the culture media at 8 μ g/mL and then the cells were pipetted. Subsequently, 100 μ L of pKLV2-U6gRNA5(gGFP)-PGKBFP2AGFP-W virus were added, and the cells were mixed well and incubated for 24 hours at 37°C in 5% CO₂. After 1 day, the culture media was changed to fresh media. The transduced cells were cultured at a density between 2-10 x 10⁵ cells/mL. After 4 days, the cells were analyzed using flow cytometry. To calculate the functional efficacy of the Cas9 in cells, the following equation was used.

$$100 - \left(\frac{\text{GFP and BFP positive cells, \%}}{\text{BFP positive cells, \%}} * 100 \right)$$

2-7-2. Amplification of library

The Human Improved Genome-wide Knockout CRISPR Library was added at a concentration of 20 ng into 25 μ L of Endura Electrocompetent cells (Lucigen, #LU60242-1). The mixture was transferred to Gene Pulser MicroPulser Cuvette (Bio-rad, #1652089). The electrocompetent cells were electroporated using Gene Pulser Xcell Total Electroporation System (Bio-rad, #1652660) at 1800 volt, 600 Ω and 10 μ F. The pulsed Electrocompetent cells were diluted with 1 mL of LB media twice and collected them. For recovery, the cells were incubated at 300 rpm at 37°C for 1 hour. 2 mL of the electroporated cells were plated on the LB agar with ampicillin in 245 mm x 245 mm square dish (SPL, #11245). To calculate electroporation efficiency, 100 μ L of 10000-fold diluted electroporated cells were plated. Each dish was incubated at 37°C for 14 hours. Colonies in each square dish were scraped twice with 10 mL of LB media. The harvested colonies were carried out maxiprep of the amplified sgRNA library by using the NucleoBond Xtra Maxi EF kit (Macherey-Nagel, #740424.50) as follows. The cells were centrifuged at 4500 g for 15 min at 4°C. The supernatant was discarded, and the cells were resuspended in 24 mL of buffer RES-EF. The resuspended cells were

divided in half and added 12 mL of buffer LYS-EF. The mixture was mixed gently by inverting five times and incubated at room temperature for 5 min. During the incubation, a column filter was equilibrated by adding 45 mL of buffer EQU-EF. Buffer NEU-EF was added into the mixture, mix gently by inverting until the blue color turned colorless completely and the mixture was incubated for 5 min in ice. After the incubation, the mixture was inverted five times and applied to the column filter. 10 mL of buffer FIL-EF was added to the column filter and then the column filter was discarded. After applying 90 mL of buffer ENDO-EF, 45 mL of buffer WASH-EF was added. The plasmid DNA was eluted with buffer ELU-EF and collected. 10.5 mL of isopropanol was mixed with eluted plasmid, vortexed and centrifuged at 15000 g for 30 min at 4°C. The supernatant was discarded, 70% ethanol was added to the pellet and centrifuged at 15000 g for 5 min at room temperature. The supernatant was removed completely and then the pellet was dried at room temperature. The dried DNA pellet was dissolved in 800 µL buffer of H₂O-EF and the concentration of plasmid was quantified.

2-7-3. NGS sequencing of amplification of library and analysis of sequencing data

For PCR of sgRNA of the amplified library, 10 forward primers and 1 barcode primer (Table 2-1) were prepared. PCR was performed with 20ng of template as described (Table 2-2 and 2-3). The PCR products were quantified and run electrophoresis on 2% agarose gel. The PCR products were gel extracted as 2-5 of the method. The gel-extracted samples were pooled at 30ng each. The pooled sample was sequenced (Theragen Bio). The sequencing data was analyzed with *count_spacer.py*.

2-7-4. Library lentivirus production

As 2-7 of the method, lentivirus was produced using Transit-293, pMD2.G, psPAX2 and Amplificated Human Improved Genome-wide Knockout CRISPR Library.

2-7-5 Library lentivirus transduction

All experiments were performed in triplicate independently using the same lentiviral library.

To 30-45% of the transduction efficiency, virus titration was required. For virus titration, 1×10^5 cells of Cas9 Jurkat were seeded at a 12-well plate in R-10 with 8 $\mu\text{g/mL}$ of polybrene.

In each well, library lentivirus was transduced at concentrations of 1, 2, 5, 10, 20 μ L. The media was changed the next day. After 4 days, the cells were analyzed using flow cytometry. The amount of virus for 45% of the transduction efficiency was calculated, 2×10^8 cells of Cas9 Jurkat was transduced at a concentration of 2×10^5 cells/mL with 8 μ g/mL of polybrene. After 24 hours, the culture soup was changed to fresh R-10. After 4 days, the transduction efficiency was analyzed using flow cytometry.

2-7-6 Genome-wide CRISPR knockout screening

Samples in our study consisted of five groups: No activation, control Ig-treated CD69⁺, control Ig-treated CD69⁻, VSIG4 Ig-treated CD69⁺ and VSIG4 Ig-treated CD69⁻. The no activation group was used to control for sgRNA enrichment. The control Ig-treated CD69^{+/+} groups were utilized to demonstrate sgRNA enrichment based on the expression of CD69. The VSIG4 Ig-treated CD69⁺ exhibits enrichment of sgRNAs that induced impaired T cell inhibition function of VSIG4. The VSIG4 Ig-treated CD69⁻ group was used to reduce noise on screening by excluding genes overlapping with the VSIG4 Ig-treated CD69⁺ group. A week after the library transduction, 1×10^8 cells were prepared for the no activation group and 2×10^8 cells each

were prepared for the activated group (control Ig-treated group and VSIG4 Ig-treated group). sgRNA⁺ Cas9 Jurkat was activated as 2-3 of the method. The cells were harvested each in a 150T flask and quantified the cell numbers. The harvested cells were centrifuged at 300 g for 3 min. The cell pellet of no activation group was stored at -80°C. The pellet of the activated group was resuspended with PBS at a concentration of 1×10^7 cells/mL. The resuspended cell was stained by CD69 monoclonal antibody (eBioscience, #12-0699-42) at a concentration of 5 μ L / 100 μ L of PBS for 30 min at 4°C. The cells were sorted in two groups by CD69 expression (CD69⁺ and CD69⁻). The sorted cells were centrifuged at 300 g for 3 min at 4°C. The pelleted cells were stored at 80°C.

2-7-7 gDNA purification

gDNA purification was performed using Quick-DNA Midiprep Plus Kit (Zymo Research, #D4075). The pelleted cells were resuspended in PBS at a concentration of 3×10^7 cells/mL. Red buffer was added to the same volume of sample, and proteinase K (Invitrogen, #25530049) was added to 30 μ L / 1 mL of sample. The mixture was vortexed for 15 second and then incubated at 55°C for 2 hours. After the incubation, Genomic lysis buffer was added to the

digested sample at the same volume of the digested sample. Zymo-Spin™ V-E Column /Reservoir was placed in a 50 mL tube. The sample was transferred into the column and centrifuged at 1,000 g for 5 min. Flow through was discarded, 9 mL of DNA Pre-Wash Buffer was added in the column and centrifuged at 1,000 g for 5 min. Flow through was discarded, 7 mL of g-DNA Wash Buffer was added in the column and centrifuged at 1,000 g for 5 min. The reservoir was removed, and the column was placed into a collection tube. The column was centrifuged at 12,000 g for 1 min and transferred into a new tube. 200 µL of g-DNA Wash Buffer was added to the column and centrifuged at 12,000 g for 1min. The column was transferred to 1.5 mL microcentrifuge tube and 200 µL of DNA Elution Buffer was added to the column. After the incubation for 5 min, the tube was centrifuged at 12,000 g for 1 min. The eluted DNA was quantified and stored at – 20°C.

2-7-8 sgRNA amplification and purification

For amplification of the sgRNA region from the extracted gDNA, 10 forward primers and a reverse primer containing the barcode sequence (Table 2-1) were prepared. A PCR was performed with at least 1.5µg of the template as described (Table 2-2 and 2-3). The amplified

sgRNAs were quantified and run electrophoresis on a 2% agarose gel. The amplified sgRNAs were gel extracted as 2-5 of the method.

2-7-9 NGS sequencing

The gel-extracted samples were pooled at equal concentration. The pooled sample was sequenced (Theragen Bio).

2-7-10 Sequencing data analysis

2-7-10-1 Counting of sgRNA, and ranking genes associated with enriched sgRNA

The sequencing data was analyzed using Python code in Model-based Analysis of Genome-wide CRISPR/Cas9 Knockout (MAGeCK) program²⁷. For selecting significantly enriched sgRNAs, the sgRNAs in CD69^{+/+} in the control Ig or the VSIG4 Ig-treated sample were normalized with the no activation sample. The genes associated with enriched sgRNAs were ranked using robust ranking aggregation (RRA) algorithm model of MAGeCK.

2-7-10-2 Validation of CRISPR screening quality

In this screening, the samples were divided based on the expression of CD69, a T cell early activation marker. Therefore, the presence of TCR signaling regulator genes in the top rank of each sample that the CRISPR screening proceeded as intended. Enriched pathways of the ranked genes in each sample were analyzed by KEGG package in R. For statistically significant and visualization of the enriched pathways, Gene Set Enrichment Analysis (GSEA) was used.

2-7-10-3 Investigation of VSIG4-mediate T cell inhibition mechanism

For the selection of the genes associated with the VSIG4-mediate T cell inhibition mechanism, the top rank genes of CD69⁺ of the VSIG4-treated group in each experiment were filtered by p-value (≤ 0.05). To reduce screening noise, the overlapping genes between the VSIG4 Ig-treated CD69⁺ and CD69⁻ groups were filtered out. In triplicate experiments, we selected genes that were replicated at least twice in filtered CD69⁺ of the VSIG4-treated group. For pathway analysis of these genes, Reactome and String were used.

Table 2-1. Primer sequences for amplification of sgRNAs of library

Primer (F/R)	Sequence (5' - 3')
F1	AATGATACGGCGACCA ^{CCGAGA} TCTACACTCTTTCCCTACAGACGCTTCCGATCTTAAGTAGAGGCTTTATATACTTTGTGAAAAGGACGAAACACACC
F2	AATGATACGGCGACCA ^{CCGAGA} TCTACACTCTTTCCCTACAGACGCTTCCGATCTAATCAATGCTTAGCTTTATATACTTTGTGAAAAGGACGAAACACACC
F3	AATGATACGGCGACCA ^{CCGAGA} TCTACACTCTTTCCCTACAGACGCTTCCGATCTGATGCACATCTCTTTTATATACTTTGTGAAAAGGACGAAACACACC
F4	AATGATA ^{CGGCGACCA} ^{CCGAGA} TCTACACTCTTTCCCTACAGACGCTTCCGATCTCGAATGCTCGACGCTTTTATATACTTTGTGAAAAGGACGAAACACACC
F5	AATGATACGGCGACCA ^{CCGAGA} TCTACACTCTTTCCCTACAGACGCTTCCGATCTTCGGATAGCAAATTCGGCTTTATATACTTTGTGAAAAGGACGAAACACACC
F6	AATGATACGGCGACCA ^{CCGAGA} TCTACACTCTTTCCCTACAGACGCTTCCGATCTATCGATAGTTGCTTGTCTTTATATACTTTGTGAAAAGGACGAAACACACC
F7	AATGATACGGCGACCA ^{CCGAGA} TCTACACTCTTTCCCTACAGACGCTTCCGATCTGATCGATCCAGTTAGGCTTTTATATACTTTGTGAAAAGGACGAAACACACC
F8	AATGATACGGCGACCA ^{CCGAGA} TCTACACTCTTTCCCTACAGACGCTTCCGATCTCGATCGATTTGAGCCTGCTTTTATATACTTTGTGAAAAGGACGAAACACACC
F9	AATGATACGGCGACCA ^{CCGAGA} TCTACACTCTTTCCCTACAGACGCTTCCGATCTACGATCGATACACGATCGCTTTTATATACTTTGTGAAAAGGACGAAACACACC
F10	AATGATACGGCGACCA ^{CCGAGA} TCTACACTCTTTCCCTACAGACGCTTCCGATCTTACGATCGATGGTCCAGAGCTTTTATATACTTTGTGAAAAGGACGAAACACACC
R1	CAAGCAGAAAGCGGCATACGAGAT TCCGCTTG GTGACTGGAGTTACAGCGTGTGCTTCCGATCTCCGACTCCGACTCGGTGCCACTTTTTTCAA (Bold = barcode)

Table 2-2. PCR master mix for amplification of sgRNAs in library

Material	Amount per Reaction (μ L)
NEBNext High Fidelity PCR Master Mix, 2 \times	25
Forward primer (1~10)	1.25
Reverse primer	1.25
sgRNA library template	X
DW	Up to 50

Table 2-3. Cycling condition for PCR

Stage	Temperature	Cycle	Time
Initial denaturation	98°C	1	3 min
Denaturation	98°C	22	10 sec
Annealing	60°C	22	10 sec
Extension	72°C	22	25 sec
Final extension	72°C	1	2 min
Hold	4°C	1	Infinite

3. Result

3-1. Establishment of functional Cas9-expressing Jurkat cell line

For CRISPR screening, the Cas9 gene was transduced into Jurkat cell line using lentiCas9-

Blast vector. Cas9 expression in the Jurkat cell was confirmed by western blot (Fig. 3-1A).

The functional efficacy of Cas9 was investigated by transducing pKLV2-U6gRNA5(gGFP)-

PGKBFP2A GFP-W into the Cas9 Jurkat cells. After 4 days, the transduced cells were

analyzed by flow cytometry. The expressed gGFP forms an RNP complex with Cas9 in the

Cas9 Jurkat to perturbate the GFP gene. BFP expressing cell has functional Cas9, whereas

BFP and GFP expressing cell have dysfunctional Cas9. The percentage of functional Cas9-

expressing cells was about 98.2% (Fig. 3-1B). Mycoplasma test of Cas9 Jurkat was negative

(Fig. 3-1C). Cas9 Jurkat cells were activated for 8 hours with a concentration of 1 $\mu\text{g}/\text{mL}$ of

anti-CD3 in the presence of VSIG4 Ig and F(ab')₂, which showed to effectively inhibit CD69

expression on T cells (Fig. 3-1D).

3-2. Amplification of human genome-wide CRISPR knockout

library

The amplification was performed to maintain and validate the human improved genome-wide knockout CRISPR library. The sgRNA library-transduced competent cells were spread onto 245-mm LB square plates. 10000-fold diluted cells were plated onto a LB agar in a 60 π dish to validate electroporation efficacy. The plates and the dish were incubated at 37°C for 14 hours and the colonies of the 10000-fold diluted cells were counted (Fig. 3-2A). The count was more than 100, which is the minimum transformation efficiency. The cells in square dishes were harvested, and maxiprep was performed to obtain an amplified sgRNA library (Fig. 3-2B). A library PCR was carried out using 10 forward primers and a reverse primer to determine the distribution of sgRNA by NGS sequencing (Fig. 3-2C). The amplicons were pooled at the same concentration and sequencing was performed. The sequencing data was analyzed using *count_spacers.py*. Generally, a sgRNA library should contain a minimum of 70% perfectly matching guides and have a skewed ratio below 10. The analyzed data revealed the total of 60,932,518 guide read, with 53,600,191 perfect matches and 5,561,650 nonperfect matches.

In the library, 90.6% of sgRNAs matched perfectly, 1.1% of sgRNAs were undetected, and the skew ratio of sgRNAs was 9.2 (Fig. 3-2D).

3-3. Enriched sgRNA amplification of activated sgRNA⁺ Cas9

Jurkat cell

For the genome-wide CRISPR knockout screening, the amplified sgRNA library was transduced into Cas9 Jurkat cells at a multiplicity of infection 0.3 (Fig. 3-3A). The sgRNA-transduced Cas9 Jurkat cells were cultured for 4 days and then sorted based on BFP expression (Fig. 3-3B and C). The sgRNA⁺ Cas9 Jurkat cells were cultured for 7 days for sufficient indel formation. One week after the transduction, 1×10^8 cells were prepared for the no activation group and 2×10^8 cells each was prepared for the activated group (control Ig-treated group and VSIG4 Ig-treated group). The activated cells were sorted based on CD69 expression (Fig. 3-3D). The purity of the sorted cells was more than 95% (Fig. 3-3E). The genomic DNA was

harvested from each sample and then the enriched sgRNAs were amplified (Fig. 3-3F). The amplicons were pooled at the same concentration and then analyzed.

3-4. Control Ig-treated group showed enrichment of sgRNAs associated with TCR signaling regulators

First, the number of sgRNAs in each sample was counted using MAGeCK tool. The enriched sgRNAs were then ranked by the RRA algorithm. Next, the analyzed data was visualized using MAGeCKFlute (Fig. 3-4A). To investigate whether the sgRNAs influenced CD69 expression, we examined the top genes in the control Ig-treated group. The control Ig-treated CD69^{+/-} group showed enrichment of TCR pathway-associated genes (Fig. 3-4B). The top-ranked genes of the positive rank in the control Ig-treated CD69⁻ group and the top-ranked genes of the negative rank in the control Ig-treated CD69⁺ group showed TCR signaling regulators included ZAP70, LAT, LCK, SLP76, and CD3 ζ . These are well-known TCR signaling regulators²⁸ (Fig 3-4C).

3-5. CRISPR screening reveals candidate genes of T cell inhibition mechanism of VSIG4

Since VSIG4 can inhibit the expression of CD69 through the activation of T cells, the top-ranked genes in the VSIG4 Ig-treated CD69⁺ group are associated with the VSIG4 signaling mechanism. We initially validated whether the sgRNA was enriched in a manner that could induce CD69 expression. The genes with depleted sgRNAs in this group (FDR ≤ 0.25) have many positive regulators of the TCR pathway (Fig. 3-5A). Next, to investigate the genes associated with the inhibitory function of VSIG4 in T cells, we selected the overlapping top-rank genes from three separate experiments. We filtered each dataset by p-value (≤ 0.05) and the selected genes that did not overlap with the top genes (p-value ≤ 0.05) in the VSIG4 Ig-treated CD69⁻ group, which are not associated with the T cell inhibitory function. The filtered data revealed the total of 223 overlapping genes, with 29 in the triple hit and 194 in the double hit (Fig. 3-5B). To find the enriched pathways of the overlapping genes, we analyzed them using Reactome (p-value ≤ 0.05). The enriched pathway of the overlapping genes showed rRNA-related pathways including rRNA processing in the nucleus and cytosol, a major pathway of rRNA processing in the nucleolus and cytosol, rRNA processing and rRNA

modification in the nucleus and cytosol (Table 3-1). Finally, to identify the candidate genes involved in the VSIG4 signal transduction mechanism associated with T cell activation, we ranked the triple hit-overlapping genes (Table 3-2) and investigated their functions related to T cell activation. This result showed that the 7 genes (PDCD2, eIF3 subunit E, eIF3 subunit F, CD5, CDK6, PCBP1 and S1PR1) may be related to the VSIG4-mediated T cell inhibition mechanism.

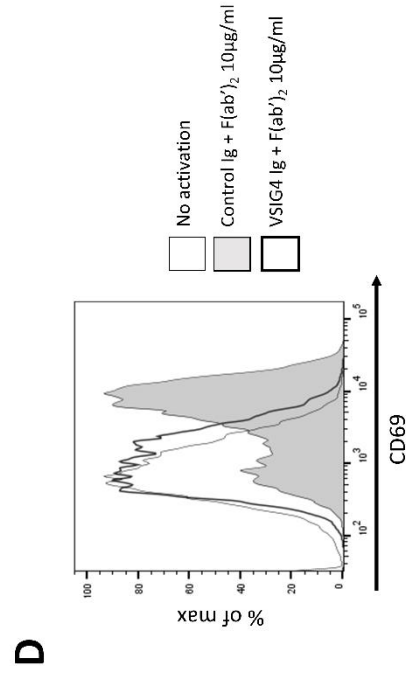
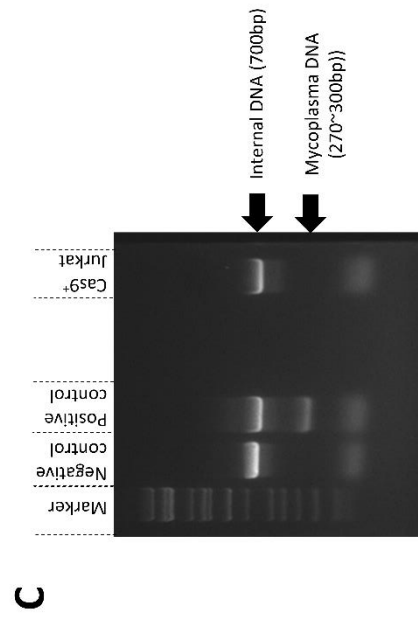
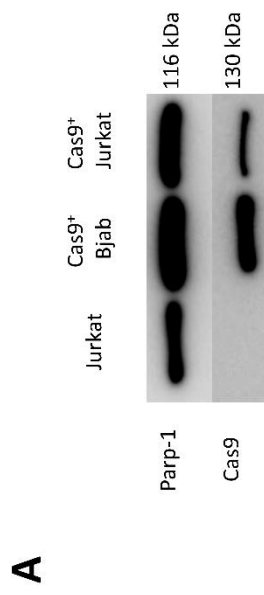
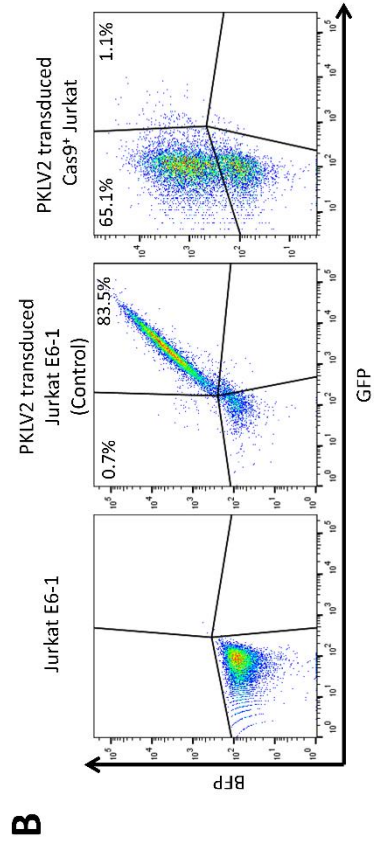


Figure 3-1. Establishment of functional Cas9-expressing Jurkat cell line. (A) Western blot of Cas9 expression of Cas9 transduced Jurkat. Jurkat cell was used as a negative control, and Cas9-expressing Bjab cell was used as a positive control. (B) The functional test of Cas9 in the Cas9 transduced Jurkat using pKLV2-U6gRNA5(gGFP)-PGKBFP2AGFP-W. Only BFP⁺ cells have functional Cas9 due to knockout of the GFP gene by gGFP. (C) Mycoplasma test of Cas9 transduced Jurkat. (D) CD3 activation for 8 hours of the Cas9 transduced Jurkat cells with super-engaged control Ig or VSIG4 Ig. VSIG4 Ig-treated population showed inhibition of CD69 expression, T cell early activation marker.

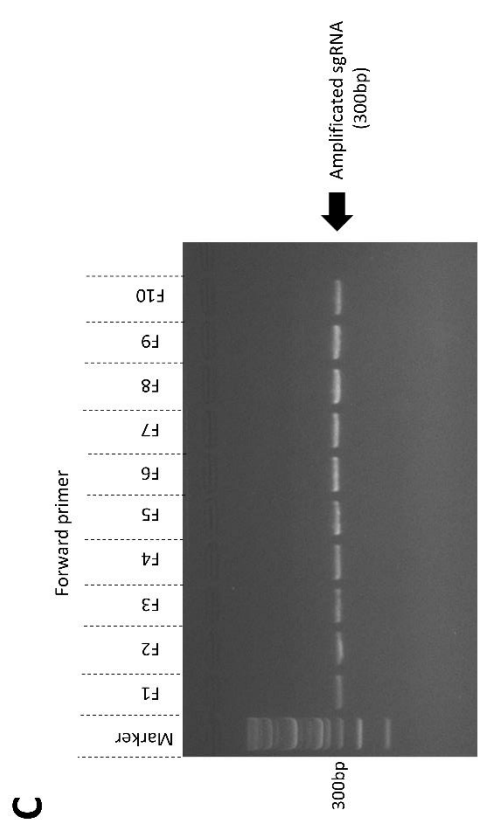
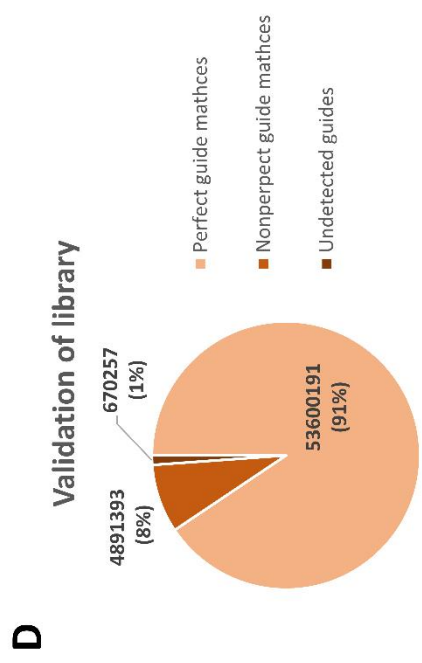
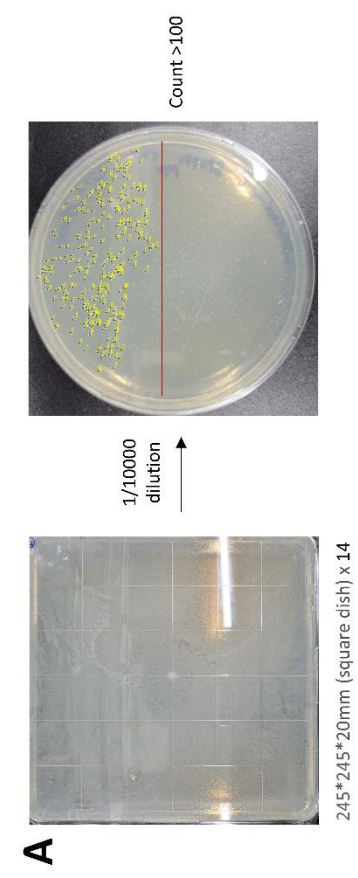
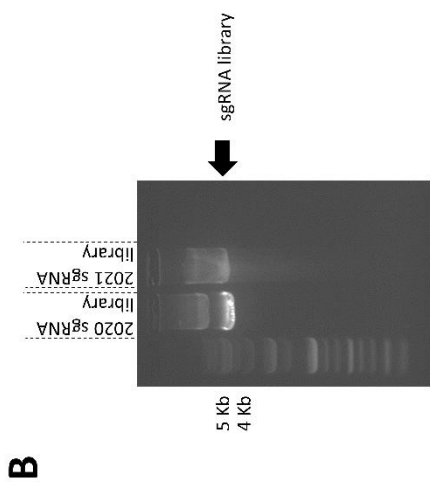
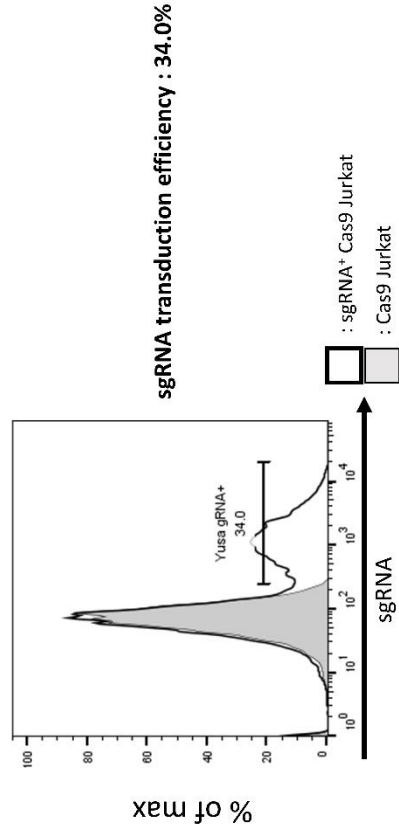
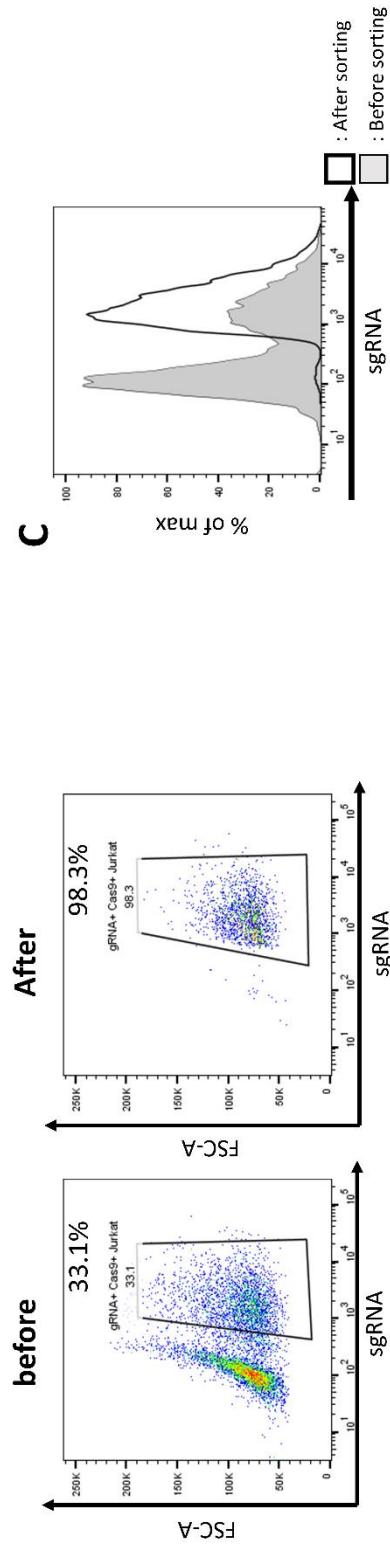


Figure 3-2. Amplification of human genome-wide CRISPR knockout library. (A) Validation of Human Improved Genome-wide Knockout CRISPR Library transformation efficacy. The colony of 10000-fold diluted cells was counted by image J software. The count was more than 100, which is the minimum transformation efficiency. (B) Electrophoresis result of the sgRNA library plasmid. (C) Electrophoresis result of the amplified sgRNA in the library. The sgRNA in the library were amplified using 10 forward primer and a barcode primer. (D) Analysis result of NGS sequencing data using count.py code. The data indicated that 90.6% of sgRNAs were matched perfectly, and 1.1% of sgRNAs were undetected.

A



B



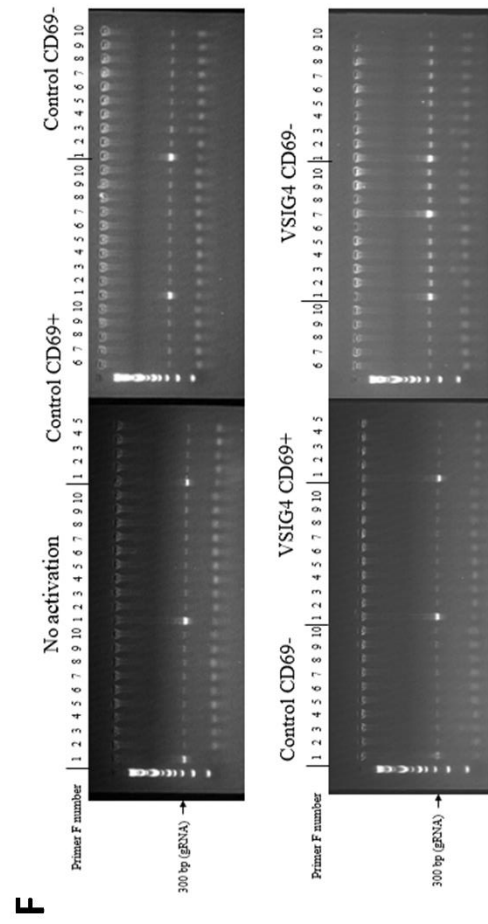
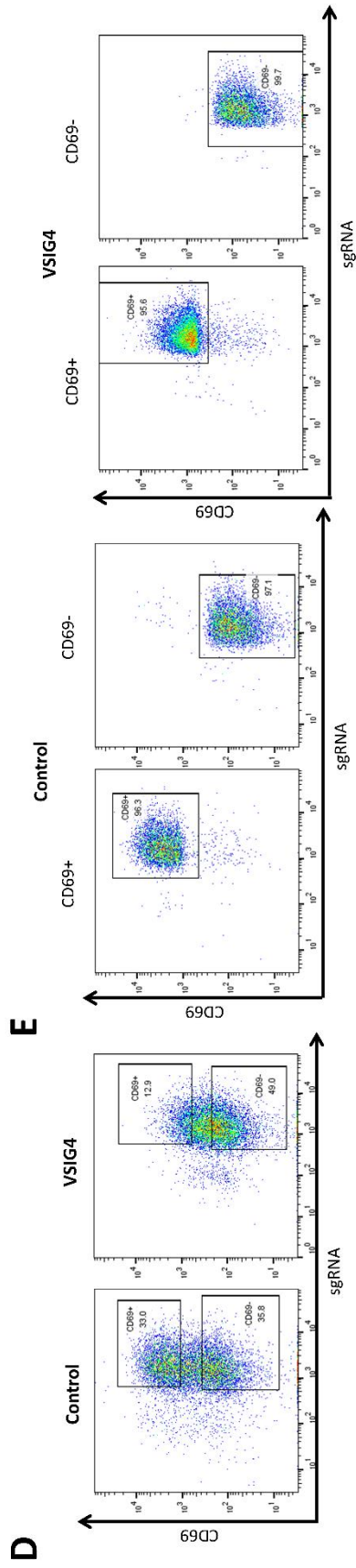


Figure 3-3. Enriched sgRNA amplification based on CD69 expression on activated sgRNA⁺ Cas9 Jurkat cell. (A) Cas9 Jurkat cells were transduced with sgRNA packaged lentivirus at MOI 0.3. (B) sgRNA⁺ Cas9 Jurkat cells were sorted and verified. To scale up the screening, the sgRNA⁺ Cas9 Jurkat cells was sorted by BFP expression and cultured up to 2 x 10⁸ cells. (C) Comparison of before and after sorting using the histogram. (D) Activated sgRNA⁺ Cas9 Jurkat cells with super-engaged control Ig or VSIG4 Ig were sorted by CD69 expression. (E) The sorted cells showed purity of more than 95%. (F) The gDNA of the samples were isolated and the sgRNA was amplified for sequencing. The sgRNAs in the samples were amplified using 10 forward primers and a barcode primer.

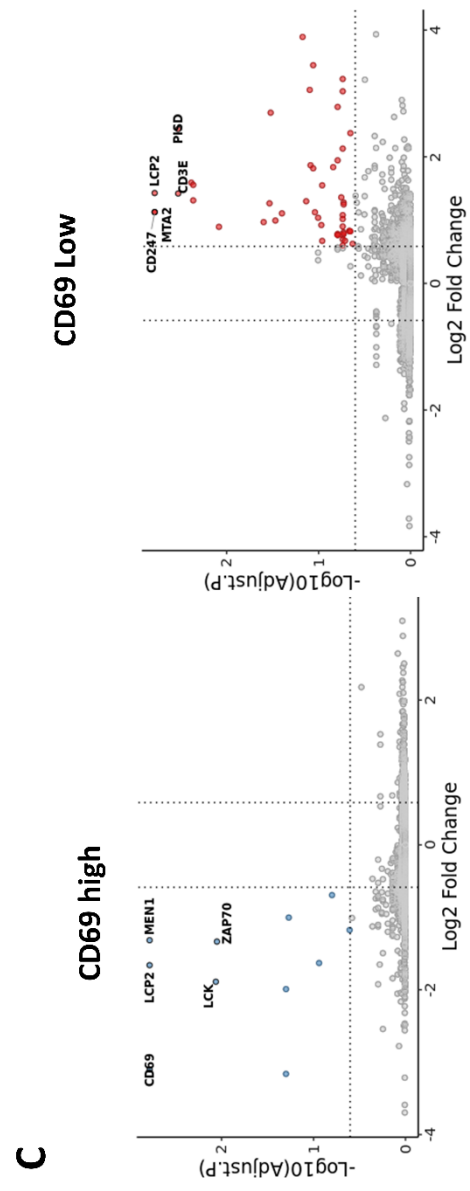
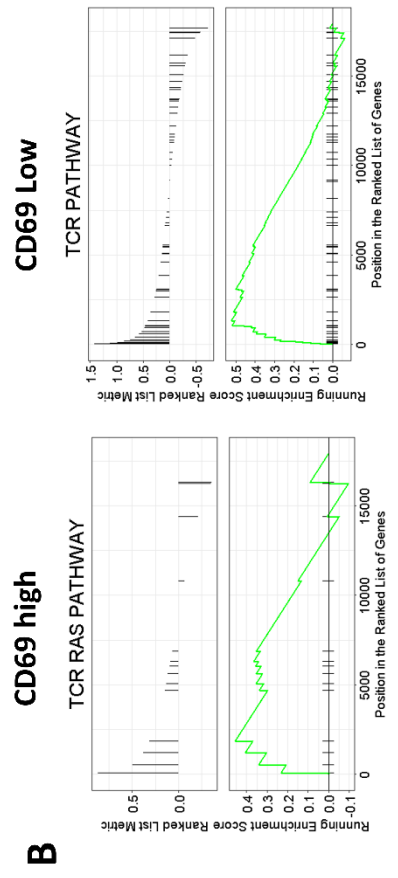
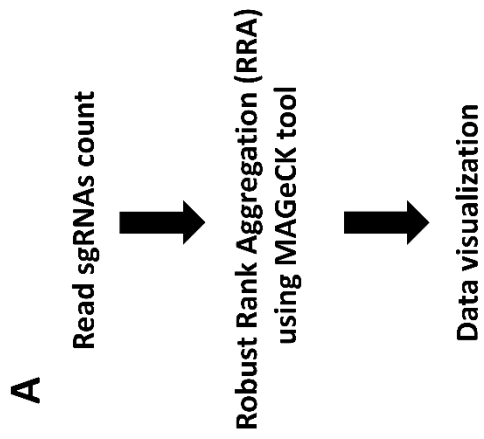
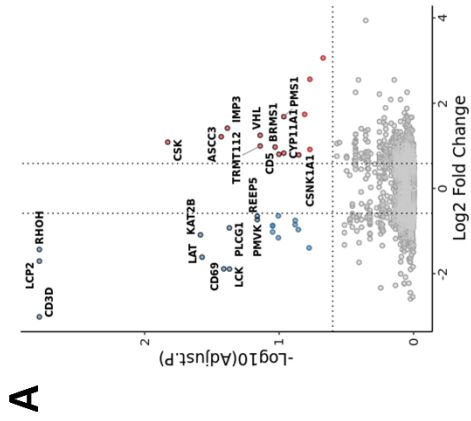


Figure 3-4. Control Ig-treated group showed enrichment of sgRNAs associated with TCR signaling regulators. (A) Analysis method of CRISPR knockout screening data. The no activation group was used as a control for the sgRNA enrichment. The genes associated with the enriched sgRNAs were ranked using the RRA function in the MAGeCK tool. The rank, p-value, and FDR of the genes were visualized using the MAGeCKFlute package in R. (B) GSEA analysis of the control Ig-treated group. The TCR pathway-associated genes were enriched. (C) Volcano plot of gene with enriched sgRNAs in the control CD69^{+/-} group (FDR < 0.25 and p-value < 0.05). The plot showed significantly enriched or depleted TCR signaling-associated genes.



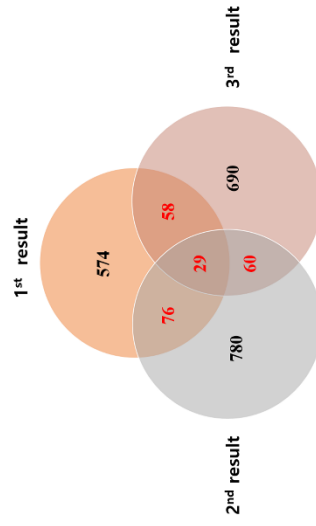
B

P value

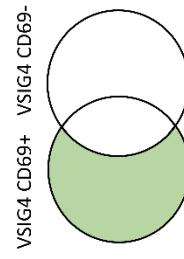


Overlapped gene selection
in triplicated experiment

Comparison
in VSIG4 treated group



Filtered top hit gene : 2601



Filtered top hit gene : 2267

Cut by
P value ≤ 0.05

Overlapped genes : 223

Figure 3-5. CRISPR screenings revealed candidate genes of T cell inhibition mechanism of VSIG4. (A) Volcano plot of genes with enriched sgRNAs in the VSIG4 Ig-treated CD69⁺ group. (FDR < 0.25 and p-value < 0.05). The plot showed a significant depletion of the TCR signaling-associated genes. The genes that induced impaired T cell inhibition function of VSIG4 were enriched. (B) Method for data filtering. To reduce screening noise, each dataset was filtered by p-value (< 0.05). The VSIG4 Ig-treated CD69⁻ group was used for excluding the genes overlapping with the VSIG4 Ig-treated CD69⁺ group. The Venn diagram of filtered genes showed a list of overlapping genes. The overlapping genes indicated that the genes were associated with the T cell inhibition mechanism of VSIG4.

Table 3-1. Enriched pathway of VSIG4 Ig-treated CD69⁺ group

Rank	Pathway name	#Entities found	#Entities total	Entities pValue
1	rRNA processing in the nucleus and cytosol	76	208	<=0.001
2	Major pathway of rRNA processing in the nucleolus and cytosol	70	189	<=0.001
3	rRNA processing	77	246	<=0.001
4	rRNA modification in the nucleus and cytosol	32	72	<=0.001
5	Ribosomal scanning and start codon recognition	28	64	<=0.001
6	Formation of the ternary complex, and subsequently, the 43S complex	25	54	<=0.001
7	Translation initiation complex formation	27	62	<=0.001
8	Activation of the mRNA upon binding of the cap-binding complex and eIFs, and subsequent binding to 43S	27	66	<=0.001
9	NoRC negatively regulates rRNA expression	28	80	<=0.001
10	GTP hydrolysis and joining of the 60S ribosomal subunit	37	120	<=0.001
11	TP53 Regulates Transcription of DNA Repair Genes	29	86	<=0.001
12	Cap-dependent Translation Initiation	38	130	<=0.001
13	Eukaryotic Translation Initiation	38	130	<=0.001
14	Formation of a pool of free 40S subunits	32	106	0.001
15	L13a-mediated translational silencing of Ceruloplasmin expression	35	120	0.001
16	Negative epigenetic regulation of rRNA expression	28	89	0.001
17	RNA Polymerase I Transcription Termination	14	33	0.002
18	SARS-CoV-1 modulates host translation machinery	16	41	0.002
19	Metabolism of RNA	164	789	0.002
20	Tristetraprolin (TTP, ZFP36) binds and destabilizes mRNA	9	19	0.005
21	RNA Polymerase I Transcription Initiation	17	50	0.005
22	Deadenylation-dependent mRNA decay	20	65	0.007
23	RNA Polymerase I Promoter Escape	19	61	0.008
24	Activation of the pre-replicative complex	13	36	0.008
25	Butyrate Response Factor 1 (BRF1) binds and destabilizes mRNA	8	19	0.015
26	SRP-dependent cotranslational protein targeting to membrane	30	119	0.018
27	PERK regulates gene expression	13	42	0.026

28	Epigenetic regulation of gene expression	33	139	0.029
29	ATF4 activates genes in response to endoplasmic reticulum stress	11	34	0.029
30	RNA Polymerase I Promoter Clearance	22	85	0.030
31	Nonsense Mediated Decay (NMD) independent of the Exon Junction Complex (EJC)	25	101	0.035
32	RNA Polymerase I Transcription	22	87	0.037
33	Synthesis of diphthamide-EEF2	6	15	0.041
34	Interleukin-37 signaling	11	36	0.041
35	Formation of HIV-1 elongation complex containing HIV-1 Tat	13	46	0.047
36	Response of EIF2AK4 (GCN2) to amino acid deficiency	27	115	0.049
37	Signaling by FGFR2 IIIa TM	8	24	0.050

Table 3-2. The positive rank of triple hit genes in VSIG4 Ig-treated CD69⁺ group

Total rank	Genes	1 st rank	2 nd rank	3 rd rank	mean
1	PDCD2	23	6	1	10
2	PELO	25	41	76	47
3	SRRD	18	57	86	54
4	EIF3H	114	24	41	60
5	PRRC2C	84	28	74	62
6	BRMS1	6	185	14	68
7	CD5	7	174	56	79
8	BRD1	45	271	6	107
9	PCBP1	245	80	20	115
10	EIF3F	261	70	185	172
11	ASUN	134	208	188	177
12	ISL2	435	45	53	178
13	VPS8	59	90	400	183
14	HEATR1	157	269	192	206
15	C7orf26	513	105	4	207
16	CNOT1	529	162	79	257
17	FBXO11	411	136	322	290
18	CDK6	332	176	463	324
19	RREB1	587	145	260	331
20	S1PR1	228	791	12	344
21	CHP1	497	366	279	381
22	GCN1L1	975	233	73	427
23	FH	714	15	889	539
24	ADSL	516	917	246	560
25	NELFA	657	237	847	580
26	DPH5	455	638	757	617
27	AKAP10	789	601	529	640
28	POLE4	233	830	884	649
29	DDI2	948	707	623	759

4. Discussion

We established a novel method to investigate the T cell inhibition mechanism of immune checkpoint molecules using genome-wide CRISPR knockout screening. The genome-wide CRISPR knockout library was transduced into Cas9-expressing Jurkat cells, which were then activated with anti-CD3 in the presence of VSIG4 Ig or control Ig. The activated T cells were sorted by CD69 expression.

Because our screening relied on the phenotype of cells, the screening power was lower than proliferation-based screening. To overcome this limitation, we increased the culture scale and performed data filtering to improve the significance of this screening.

Our data demonstrated that the sgRNAs targeting positive regulators of TCR signaling, including ZAP70, SLP76, LCK, and CD3 subunits, were enriched in the CD69⁻ population, while these sgRNAs were depleted in the CD69⁺ population. The results showed that the CRISPR screening proceeded as intended. In the VSIG4 Ig-treated group, we utilized the

CD69⁺ population to explore the genes implicated in the signal transduction mechanism of VSIG4. We used the CD69⁻ population to demonstrate the enrichment of sgRNAs based on the expression of CD69 and to exclude the genes that are not relevant to VSIG4 signaling. To investigate the pathways associated with VSIG4 signaling, we analyzed the overlapping genes using the pathway analyzer, Reactome. The top-ranked pathways were associated with ribosomal RNA processing. Because rRNA processing is related to T cell activation²⁹, this result showed a significant association between the ribosomal RNA-related pathway and the T cell inhibitory function of VSIG4. Additionally, to find the genes directly involved in the VSIG4 signal transduction mechanism, we focused on finding the genes related to T cell activation in the triple hit genes using gene ontology. Among these genes, PDCD2 (Rank 1), eIF3 subunit E and F (Rank 4 and 10), CD5 (Rank 7), CDK6 (Rank 18), PCBP1 (Rank 19) and S1PR1 (Rank 20) were associated with T cell activation. PDCD2 is an essential gene for cell proliferation and apoptosis^{30,31}. PDCD2 is associated with BCL6, which is related to the stability of Treg and the induction of CD8 T cell activation^{32,33}. Since the mechanism of PDCD2 is not yet fully understood, investigating its association with VSIG4 could provide

insight into the T cell regulatory mechanisms of PDCD2. eIF3 is a complex of 13 subunits that are required for robust T cell activation. When a T cell is activated, the eIF3 complex binds to 3'-UTR on the mRNA of TCRA and TRCB, which then induces translation of TCRA and TCRB. CD5 interacts with CSK, CBL, CBLB, UBASH3A, and UBASH3B, which are known negative regulators of TCR signaling³⁴⁻³⁷. These interaction results in T cell inhibition in mature T cells. Our data showed that VSIG4 may have the potential to enhance the T cell inhibition function through CD5. CDK6 is a regulator of the cell cycle and inhibitor of the nuclear factor of activated T cell³⁸. CDK6 inhibits the T cell activation by increasing the activity of PTP1B and protein tyrosine phosphatase, which reduces the phosphorylation of CD3 zeta³⁹. Especially, because CDK6 has been used as a target of immunotherapy, investigation of an association between CDK6 and VSIG4 may improve the efficacy of cancer immunotherapy. PCBP1 is upregulated in activated T cell and inhibits the conversion of effector T cell into regulatory T cell⁴⁰. VSIG4 has the potential to induce the conversion to Tregs by inhibiting the function of PBCP1. S1PR1, Sphingosine-1-Phosphate receptor 1, is associated with T cell differentiation. When S1PR1 is ligated with its ligand, this signaling

induces the TH1/TH17 effector phenotype and prevents the induction of Treg⁴¹. In this perspective, our data indicate that VSIG4 has the potential to induce the Treg by inhibiting S1PR1 signaling.

In this study, we provided a comprehensive understanding of the T cell inhibition mechanism of VSIG4 from various perspectives. These insights will lead to a higher efficacy of immune checkpoint blockade therapy and provide breakthroughs for immune diseases.

5. Conclusions

We established a method of genome-wide CRISPR knockout screening to investigate T cell inhibition mechanism of an immune checkpoint molecule.

In our genome-wide CRISPR knockout screening, we identified the 223 candidate genes that potentially affect the T cell inhibitory function of VSIG4. Pathway analysis revealed a significant association between the ribosomal RNA-related pathway and the T cell inhibitory function of VSIG4. Moreover, we focused on 7 promising candidate genes that play a role in the T cell inhibitory function of VSIG4.

6. References

1. Xu, Y., Chen, C., Guo, Y., Hu, S. & Sun, Z. Effect of CRISPR/Cas9-Edited PD-1/PD-L1 on Tumor Immunity and Immunotherapy. *Frontiers in Immunology* vol. 13 Preprint at <https://doi.org/10.3389/fimmu.2022.848327> (2022).
2. Wagner, M., Jasek, M. & Karabon, L. Immune Checkpoint Molecules—Inherited Variations as Markers for Cancer Risk. *Front Immunol* **11**, 1–29 (2021).
3. Waldman, A. D., Fritz, J. M. & Lenardo, M. J. A guide to cancer immunotherapy: from T cell basic science to clinical practice. *Nat Rev Immunol* **20**, 651–668 (2020).
4. Baxevanis, C. N. Immune Checkpoint Inhibitors in Cancer Therapy—How Can We Improve Clinical Benefits? *Cancers (Basel)* **15**, 3–7 (2023).
5. Gauci, M.-L. *et al.* Long term survival in patients responding to an Anti-PD-1/PD-L1 therapy and disease outcome upon treatment discontinuation. *Annals of Oncology* **28**, v411 (2017).
6. Weimer, P. *et al.* Tissue-Specific Expression of TIGIT, PD-1, TIM-3, and CD39 by $\gamma\delta$ T Cells in Ovarian Cancer. *Cells* **11**, (2022).
7. Rotte, A. Combination of CTLA-4 and PD-1 blockers for treatment of cancer. *Journal of Experimental and Clinical Cancer Research* **38**, 1–12 (2019).
8. Seidel, J. A., Otsuka, A. & Kabashima, K. Anti-PD-1 and anti-CTLA-4 therapies in cancer: Mechanisms of action, efficacy, and limitations. *Front Oncol* **8**, 1–14 (2018).
9. Larkin, J. *et al.* Combined Nivolumab and Ipilimumab or Monotherapy in Untreated Melanoma. *New England Journal of Medicine* **373**, 23–34 (2015).

10. He, X. & Xu, C. Immune checkpoint signaling and cancer immunotherapy. *Cell Res* **30**, 660–669 (2020).
11. Li, J. *et al.* VSIG4 inhibits proinflammatory macrophage activation by reprogramming mitochondrial pyruvate metabolism. *Nat Commun* **8**, (2017).
12. Helmy, K. Y. *et al.* CRIG: A macrophage complement receptor required for phagocytosis of circulating pathogens. *Cell* **124**, 915–927 (2006).
13. Liu, B. *et al.* The biology of VSIG4: Implications for the treatment of immune-mediated inflammatory diseases and cancer. *Cancer Lett* **553**, 215996 (2023).
14. Jung, K. *et al.* VSIG4-expressing tumor-associated macrophages impair anti-tumor immunity. *Biochem Biophys Res Commun* **628**, 18–24 (2022).
15. Zhou, X., Khan, S., Huang, D. & Li, L. V-Set and immunoglobulin domain containing (VSIG) proteins as emerging immune checkpoint targets for cancer immunotherapy. *Front Immunol* **13**, 1–14 (2022).
16. Widyagarini, A., Nishii, N., Kawano, Y., Zhang, C. & Azuma, M. VSIG4/CRIG directly regulates early CD8⁺ T cell activation through its counter-receptor in a narrow window. *Biochem Biophys Res Commun* **614**, 100–106 (2022).
17. Vogt, L. *et al.* VSIG4, a B7 family-related protein, is a negative regulator of T cell activation. *Journal of Clinical Investigation* **116**, 2817–2826 (2006).
18. Yuan, X., Yang, B. H., Dong, Y., Yamamura, A. & Fu, W. CRIG, a tissue-resident macrophage specific immune checkpoint molecule, promotes immunological tolerance in NOD mice, via a dual role in effector and regulatory T cells. *Elife* **6**, 1–29 (2017).
19. Kim, S. W. *et al.* Expression of the immune checkpoint molecule V-set immunoglobulin domain-containing 4 is associated with poor prognosis in patients with advanced gastric cancer. *Gastric Cancer* **24**, 327–340 (2021).

20. Liao, Y. *et al.* VSIG4 expression on macrophages facilitates lung cancer development. *Laboratory Investigation* **94**, 706–715 (2014).
21. Byun, J. M. *et al.* The significance of VSIG4 expression in ovarian cancer. *International Journal of Gynecological Cancer* **27**, 872–878 (2017).
22. Roh, J. *et al.* Expression of immune checkpoint molecule vsig4 is correlated with poor prognosis in multiple myeloma. *Pathology* **48**, S153–S154 (2016).
23. Hall, B. M. *et al.* Immune checkpoint protein VSIG4 as a biomarker of aging in murine adipose tissue. *Aging Cell* **19**, 1–17 (2020).
24. Schreurs, J. *et al.* Recent advances in crispr/cas9-based genome editing tools for cardiac diseases. *Int J Mol Sci* **22**, (2021).
25. Sanjana, N. E., Shalem, O. & Zhang, F. Improved vectors and genome-wide libraries for CRISPR screening. *Nat Methods* **11**, 783–784 (2014).
26. Tzelepis, K. *et al.* A CRISPR Dropout Screen Identifies Genetic Vulnerabilities and Therapeutic Targets in Acute Myeloid Leukemia. *Cell Rep* **17**, 1193–1205 (2016).
27. Li, W. *et al.* MAGeCK enables robust identification of essential genes from genome-scale CRISPR/Cas9 knockout screens. *Genome Biol* **15**, 554 (2014).
28. Gaud, G., Lesourne, R. & Love, P. E. Regulatory mechanisms in T cell receptor signalling. *Nat Rev Immunol* **18**, 485–497 (2018).
29. Tan, T. C. J. *et al.* Suboptimal T-cell receptor signaling compromises protein translation, ribosome biogenesis, and proliferation of mouse CD8 T cells. *Proc Natl Acad Sci U S A* **114**, E6117–E6126 (2017).
30. Baron, B. W. *et al.* The human programmed cell death-2 (PDCD2) gene is a target of BCL6 repression: Implications for a role of BCL6 in the down-regulation of apoptosis. *Proc Natl Acad Sci U S A* **99**, 2860–2865 (2002).

31. Baron, B. W., Hyjek, E., Gladstone, B., Thirman, M. J. & Baron, J. M. PDCD2, a protein whose expression is repressed by BCL6, induces apoptosis in human cells by activation of the caspase cascade. *Blood Cells Mol Dis* **45**, 169–175 (2010).
32. Yoshida, K. *et al.* Bcl6 controls granzyme B expression in effector CD8⁺ T cells. *Eur J Immunol* **36**, 3146–3156 (2006).
33. Sawant, D. V. *et al.* The transcriptional repressor Bcl6 controls the stability of regulatory T cells by intrinsic and extrinsic pathways. *Immunology* **145**, 11–23 (2015).
34. Augustin, R. C., Bao, R. & Luke, J. J. Targeting Cbl-b in cancer immunotherapy. *J Immunother Cancer* **11**, 1–16 (2023).
35. Voisinne, G., Gonzalez de Peredo, A. & Roncagalli, R. CD5, an Undercover Regulator of TCR Signaling. *Front Immunol* **9**, 1–8 (2018).
36. Ge, Y., Paisie, T. K., Chen, S., Concannon, P. & Program, C. B. UBASH3A regulates the synthesis and dynamics of T-cell receptor-CD3 complexes. **203**, 2827–2836 (2020).
37. Tan, Y. X. *et al.* Inhibition of the kinase Csk in thymocytes reveals a requirement for actin remodeling in the initiation of full TCR signaling. *Nat Immunol* **15**, 186–194 (2014).
38. Deng, J. *et al.* CDK4/6 inhibition augments antitumor immunity by enhancing T-cell activation. *Cancer Discov* **8**, 216–233 (2018).
39. Gao, X. *et al.* Targeting protein tyrosine phosphatases for CDK6-induced immunotherapy resistance. *Cell Rep* **42**, 112314 (2023).
40. Ansa-Addo, E. A. *et al.* RNA binding protein pcbp1 is an intracellular immune checkpoint for shaping t cell responses in cancer immunity. *Sci Adv* **6**, 1–16 (2020).

41. Cibrián, D. & Sánchez-Madrid, F. CD69: from activation marker to metabolic gatekeeper. *Eur J Immunol* **47**, 946–953 (2017).

Abstract (in Korean)

T세포의 활성을 조절하는 면역관문 분자(immune checkpoint molecule)를 표적으로 하는 면역치료제(immune checkpoint blockade)는 치료 효과의 높은 지속성(durability)과 안전성(stability)으로 암 치료효과의 획기적인 도약을 이루어 냈다. 그러나 낮은 치료 반응성과 암 종별 제한적인 효과를 보여주고 있어, 이를 극복하기 위한 새로운 면역치료제의 개발이 시급하다. VSIG4는 T 세포의 활성을 억제하고 조절 T 세포(regulatory T cells)로의 분화를 촉진하는 새로운 면역관문 조절자로, VSIG4의 발현이 위암과 림프종(lymphoma) 환자의 예후뿐만 아니라 노화성 면역질환과 밀접한 연관성을 갖고 있어, 새로운 면역 치료제의 개발 후보로 많은 관심을 받고 있다. 이러한 잠재력에도 불구하고, 현재까지 VSIG4의 T cell inhibition mechanism은 제대로 밝혀지지 않았다. 본 실험은 새로운 면역치료제 개발 기반 제공을 위해 VSIG4의 T 세포 활성 억제 신호기전을 genome-wide CRISPR screening을 통해 밝혀냈다. 우선, T 세포의 초기 활성화 마커(marker)인 CD69의 증감을 통해 T 세포의 활성 및 VSIG4를 통한 활성 억제를 평가할 수 있는 시험관 내(in vitro) 모델을 구축했다. 해당 모델에 genome-wide CRISPR knockout library를 삽입 한 후, CD69증가 세포군과 CD69감소 세포군을 분리(순도 >95%)하고, 각 세포군의 genomic DNA에서 guide count를 NGS를

통해 분석했다. MAGeCK-Robust Rank Aggregation을 통해 유의미한 sgRNA의 변화를 분석(p < 0.05, FDR < 0.25)하여 VSIG4의 T 세포 활성화 억제 기전 유전자 후보들을 도출하였다. Reactome과 String 분석을 통해, VSIG4가 ribosomal RNA processing과 CD5 pathway, S1PR1 pathway를 조절하여 T 세포의 활성을 억제함을 확인했다. 이 기전들은 T 세포 수용체(receptor)의 신호강도를 조절, 조절 T 세포의 분화, T 세포의 활성화 등이 연관되어 있음이 밝혀져 있다. 본 실험으로 밝혀진 VSIG4의 T 세포 활성화 억제기전을 통해 한국인에서 높게 발생하는 위암과 림프종의 치료제 개발의 기반을 제공할 수 있다. 또한, VSIG4는 기존 면역치료제와는 다른 신호기전을 통해 T세포의 활성을 억제하기 때문에 기존 면역치료제와의 병용치료를 통해 치료반응성을 크게 향상시키는 새로운 치료전략을 개발할 수 있다.